Polymer 52 (2011) 2847–2855

Contents lists available at ScienceDirect

Polymer

journal homepage: www.elsevier.com/locate/polymer

Development of layer-by-layer assembled carbon nanofiber-filled coatings to reduce polyurethane foam flammability

Yeon Seok Kim [a], Rick Davis [a,*], Amanda A. Cain [b], Jaime C. Grunlan [b]

[a] National Institute of Science and Technology, Engineering Laboratory, 100 Bureau Drive MS-8665, Gaithersburg, MD 20899-8665, USA
[b] Department of Mechanical Engineering, Texas A&M University, College Station, TX 77843-3123, USA

ARTICLE INFO

Article history:
Received 3 February 2011
Received in revised form
31 March 2011
Accepted 10 April 2011
Available online 15 April 2011

Keywords:
Layer-by-layer assembly
Carbon nanofibers
Flammability

ABSTRACT

Layer-by-layer (LbL) assemblies made with carbon nanofibers (CNFs) are shown to reduce the flammability of polyurethane foam. The 359 ± 36 nm thick four bilayer coating of polyethyleneimine/CNF (cationic layer) and poly(acrylic acid) (anionic layer) contains 51 ± 1 mass fraction % CNF. This coating completely covers the entire internal and external surfaces of the porous foam. Even though the microscopic CNF distribution was non-uniform, the macroscopic CNF network armor that was generated from this LbL process significantly reduced the flammability of the foam (e.g., 40% ± 3% reduction in peak heat release rate). Normalized by flame retardant concentration, the reduction in foam peak heat release due to these CNF coatings is 38% larger than CNF embedded in the foam and as high as 1138% greater than other commercial technologies used to reduce foam flammability.

Published by Elsevier Ltd.

1. Introduction

The estimated annual societal cost of soft furnishing (mattresses and upholstered furniture) fires to the United States economy is $5 billion [1–4]. These are among the deadliest as they account for 5% of all residential fires annually, but are responsible for a disproportionately high portion of the fire losses (33% of the civilian fatalities, 18% of civilian injuries, and 11% of the property losses). Over the next decade, federal flammability performance regulations are expected to significantly reduce these fire losses [5–7]. Soft furnishing manufactures are and will likely continue to comply with these current and proposed flammability regulations by using fire blocking barrier fabrics. Despite this compliance, engineering and technical options to comply are quickly diminishing because of mandated sustainability regulations, such as REACH [8] and EcoLabel [9], for consumer products. Using Layer-by-layer assembly to create a fire resistant armor on the components in soft furnishings is being evaluated in this project as a novel technology to enable these manufacturers to comply with flammability and sustainability regulations.

Layer-by-layer (LbL) assembly has been extensively studied for the past 20 years as a methodology to create multifunctional thin films generally less than 1 micron thick [10–12]. These thin films were commonly fabricated through alternate deposition of a positively charged layer and negatively charge layer (called a bilayer, BL). By taking advantage of electrostatic [13], H-bonding [14], covalent bonds [15], and/or donor/acceptor interactions, these bilayers were assembled on the surface of substrates. The LbL process is quite flexible and robust, which allows it to be tuned for specific coating characteristics and for coating a range of substrate types. For example, altering the concentration, pH, and/or temperature of the LbL solutions can result in a 1 nm rather than 100 nm thick BL [16,17].

LbL thin films have been used in an extensive breadth of applications, such as oxygen barriers [18] and sensors [19], and have useful properties, such as antimicrobial [20] and antireflection [21]. For more than a decade clay has been used as an additive in polymers since clay has shown to simultaneously improve the mechanical and fire performance attributes of polymers [22–24]. More recently, fabrication of clay containing LBL thin films has been studied [18,25,26]. Li et al. [12] focused on using LbL clay coatings (sodium exchanged montmorillonite) on cotton fabric to improve the fire performance characteristics of this textile, which is directly aligned with the research presented in this manuscript. Their results are exciting in that uniform high quality clay based coatings on cotton were achieved. In addition, the clay coatings resulted in a significant retention of fabric like char after conducting vertical burn tests and there was no (or less) ember afterglow when the flame was removed. These results suggest the coating may better prevent thermal and flame penetration from reaching and igniting the polyurethane foam (PUF), and therefore, a clay/cotton ticking or barrier may reduce flame spread in residential homes if used in soft furnishings.

Another additive filler that has gained increasing attention for improving the properties of polymeric materials is carbon nanofiber

* Corresponding author. Tel.: +1 3019755901; fax: +1 3019754052.
E-mail address: rick.davis@nist.gov (R. Davis).

0032-3861/$ – see front matter Published by Elsevier Ltd.
doi:10.1016/j.polymer.2011.04.023

(CNF). Carbon nanofibers (CNFs) are cylindrical nanostructures constructed of stacked graphitic cones or cups. Compared to carbon nanotube (CNT), CNF can be at least an order of magnitude larger, with a diameter and length in the range of 5 nm–300 nm and 0.1 μm–1000 μm, respectively. Due to the intrinsic electrical, thermal, and mechanical properties of CNF, the thermal and electrical conductivity, tensile and compressive strength, ablation resistance, damping properties, and flammability of polymers [27] have been significantly altered with their incorporation [28].

Zammarano recently reported a reduction in PUF flammability by the incorporation of CNFs directly into the polyurethane matrix [27]. At a CNF loading of 4 mass fraction %, the CNFs formed a network structure that reduced the peak heat release rate (PHRR) in burning PUF by 35% and prevented melt dripping, which in a real fire scenario, could result in an additional 30% reduction in PHRR [29]. The approach of incorporating CNFs into the PUF has a few potential drawbacks. For example, commercialization may be difficult, as the foam manufacturing process is quite sensitive to small changes in recipe, especially the presence of solid particles, and the manufacturing conditions. Another potential drawback is based on the mechanism by which CNFs are believed to reduce polymer flammability [30]. This reduction in flammability is believed to result from the formation of a char at the surface that thermally protects the polymer and prevents volatilization of degradation products [31]. Since the CNFs are dispersed and distributed throughout the polymer matrix, the polymer has to burn for some time before enough of the polymer is pyrolyzed that a high enough concentration of CNFs can aggregate at the surface to form the protective char layer (armor).

The research presented here is unique in that it is the first published report of fabricating carbon nanofiber (CNF) based thin films/coatings using LbL assembly, of fabricating LbL coatings on foam (polyurethane foam, PUF), and of altering the fire performance attributes of foam using this thin film techniques. The large CNF dimensions are undesirable for typical applications of LbL coatings, as the coating thickness is generally comparable to the CNF dimensions and it facilitates aggregation both in the fabrication solutions and in the coatings. However, for reducing flammability, the larger dimensions may enable the formation of a CNF network armor that protects the foam. The thin coating approach is believed to be ideal for reducing the flammability of foam as it may more quickly form the char-like armor because the high concentration of CNFs is already at the surface rather than randomly mixed throughout the polymer. Provided are the details of fabricating CNF coated polyurethane foam (CNF/PUF) using LbL, the physical characteristics of the LbL CNF coatings on PUF, and the measured fire performance of PUF and CNF/PUF.

2. Experimental section[1,2,3]

2.1. Materials

All materials were used as-received from the supplier unless otherwise indicated. Branched polyethylenimine (PEI, branched, mass average molecular mass = 25,000 g/mol) and poly (acrylic acid) (PAA, mass average molecular mass = 100,000 g/mol) were obtained from Sigma–Aldrich (Milwaukee, WI). PR-24-XT-PS carbon nanofibers (CNF, average diameter = 150 nm ± 100 nm, length was 65μm ± 30 μm) were obtained from Pyrograf Products Incorporated (Cedarville, Ohio). The standard (untreated) polyurethane foam (PUF) received from Future Foam Inc. (Fullerton, CA) was stored as-received from the supplier (cardboard box with no packaging material at 25°C ± 2 °C). On the day of coating, nine substrates (length/width//height of (10.2 cm/10.2 cm/5.1 cm) ± 0.1 cm) were cut from a single as-received substrate (length/width//height of (30.6 cm/30.6 cm/5.1 cm) ± 0.1 cm). These smaller substrates were rinsed and wringed out (discussed below in the coating process) to remove debris and other extractables (0.6 mass fraction % ± 0.1 mass fraction %). After drying, the post-extraction mass of these substrates was 12.7 g ± 0.3 g.

The polyelectrolyte (0.1 mass fraction % ± 0.03 mass fraction %) solutions were prepared by charging a glass container (2 L) with distilled water (DI, conductivity < 0.5 μS, 1300 mL) and polymer (0.10 mass fraction % ± 0.03 mass fraction %, 1.3 g ± 0.4 g) then slowly agitating for 6 h at room temperature. The pH values for the PAA anionic and PEI cationic solutions were 3 and 10, respectively. The CNF/PEI suspension in DI water was prepared by charging a plastic bottle (250 mL) with the PEI cationic stock solution (150 mL ± 1 mL) then adding CNF powder (0.050 mass fraction % ± 0.003 mass fraction % relative to total PEI stock solution (600 mL), 0.30 g ± 0.020 g). The suspension was sonicated at 40 W for 1 h with the temperature never exceeding 70°C ± 1 °C. The sonicated suspension was diluted with more PEI stock solution (450 mL) and was shaken for 3min ± 1 min. The CNF/PEI suspension was used immediately for coating the PUF.

2.2. CNF coating methodology

CNF/PUF fabrication took approximately 29 min per specimen (14 min for first bilayer and 15 min for the remaining 3 bilayers). In general, the fabrication process was alternately depositing cationic (CNF and PEI) and anionic (PAA) layers on the surface of the PUF and removing unbound material (polymer and CNF) by rinsing with DI water and wringing out the excess water several times (Fig. 1). The process of removing excess water using a convection oven and dessicator occurred over a period of 3 d.

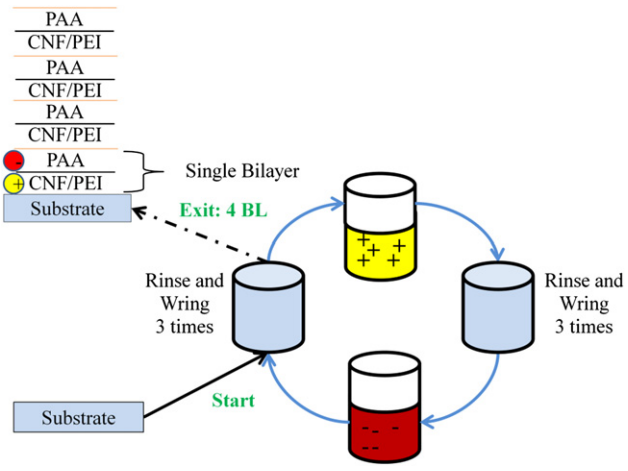

Fig. 1. The CNF/polymer coating process was an alternating submersion in a cationic (CNF/PEI) and an anionic (PAA) solution, with washing (rinse and wring) between each solution. After creating 4 bilayers (a CNF/PEI layer and a PAA layer), the specimen was dried in a convection oven for 12 h at 70°C ± 1 °C to remove excess water.

[1] Certain commercial equipment, instruments or materials are identified in this paper in order to specify the experimental procedure adequately. Such identification is not intended to imply recommendation or endorsement by the National Institute of Standards and Technology, nor is it intended to imply that the materials or equipment identified are necessarily the best available for this purpose.

[2] The policy of NIST is to use metric units of measurement in all its publications, and to provide statements of uncertainty for all original measurements. In this document however, data from organizations outside NIST are shown, which may include measurements in non-metric units or measurements without uncertainty statements.

[3] In this document, we have provided link(s) to website(s) that may have information of interest to our users. NIST does not necessarily endorse the views expressed or the facts presented on these sites. Further, NIST does not endorse any commercial products that may be advertised or available on these sites.

More specifically, a plastic container (2 L) was charged with the CNF/PEI cationic suspension (600 mL ± 10 mL), a similar container was charged with the PAA anionic solution (600 mL ± 10 mL), and six more containers were charged with deionized water (600 mL ± 10 mL each). A PUF substrate was submersed into the CNF/PEI cationic suspension and after squeezing and releasing (by hand) the substrate four times in the CNF/PEI suspensions, the substrate was soaked in the suspension for an additional 5 min. The substrate was removed and the excess solution was squeezed back into the cationic dipping container.

To remove unbound PEI and/or CNF, the substrate was thoroughly rinsed in three separate containers. Since most of the cationic materials were typically removed in the first rinsing container, the rinsing water in this container was replaced with fresh deionized water after each washing cycle. Excess water was removed by passing the substrate twice through a Dyna-Jet BL-44 hand wringer (Dyna-Jet Products, Overland Park, KS).

The PAA anionic layer was then deposited and the unbound PAA was removed using the same procedure as described above, except the washing was performed using different rinsing containers than those used for the cationic washing. This deposition of the CNF/PEI layer followed by the PAA layer created a single bilayer (CNF/PEI:-PAA). The procedure for depositing the next three bilayers was similar to the first bilayer, except the substrate was only submersed in the coating solutions for 1 min rather than 5 min. After the four bilayers were deposited, the specimen was dried in a convection oven (70°C ± 1 °C, 12 h) and stored in a dessicator (at least 3 days) with anhydrous calcium sulfate before weighing and analyzing.

2.3. CNF coating characterization

All measured values are reported with a 2σ uncertainty, unless otherwise indicated. The physical characteristics of the CNF/PUF are provided in Table 1. The increase in substrate mass due to the coating (mass fraction % coating) was measured using a laboratory microbalance. The amount of CNF in the coating (mass fraction % CNF in coating) was calculated from Thermal Gravimetric Analysis and microbalance values.

A Zeiss Ultra 60 Field Emission-Scanning Electron Microscope (FE-SEM, Carl Zeiss Inc., Thornwood, NY) was used to collect images of the CNF coatings, from which, the coating thickness was approximated (Table 1), and the distribution of CNFs and overall quality of the LbL coating was inspected. All SEM samples were sputter coated with 4 nm of Au/Pd (60 mass fraction %/40 mass fraction %) prior to SEM imaging.

A Maxtek Research Quartz Crystal Microscope (QCM, Infinicon, East Syracuse, NY), with a 3.8 MHz–6 MHz frequency range, was used in conjunction with a 5 MHz crystal to measure the mass per deposited layer. The CNF coatings were deposited onto the crystal, in its holder, using a similar procedure for coating the PUF, except no wringing, and between each layer deposition the crystal was placed on the microbalance until the measured mass stabilized (approximately 5 min).

A KLA-Tencor P-6 profilometer (KLA-Tencor, Milpitas, CA), operating at a stylus scanning rate of 20 μm/s, was used to measure the thickness of CNF coatings deposited on a glass microscope slide. The CNF coatings were deposited using the modified procedure described for QCM analysis.

A Q-500 Thermal Gravimetric Analyzer (TGA, TA Instruments, New Castle, DE) was used to measure the concentration of CNF on the substrates (Table 1, Mass fraction % CNF on CNF/PUF). The samples (15 mg ± 3 mg) were placed on a ceramic pan (250 μL, TA Instruments) then loaded into the furnace by the autosampler. Under a nitrogen atmosphere, the temperature was stabilized at 90°C ± 1 °C (30 min) then ramped to 800°C ± 2 °C at 10 °C/min. The reported CNF content was based on the remaining mass fraction % at 600 °C.

A dual Cone Calorimeter (Fire Testing Technology, East Grinstead, United Kingdom), operating at 35 kW/m^2 with an exhaust flow of 24 L/s, was used to measure the fire performance of uncoated and CNF coated PUF. The experiments were conducted according to standard testing procedures (ASTM E–1354-07). A ((10.2 cm/10.2 cm/5.1 cm) ± 0.1 cm) sample was placed in a pan constructed from aluminum foil. The pan sides were 1 cm ± 0.1 cm tall and slightly flared away from the sample to allow for all the sides and the top surface to be exposed during the test. The standard uncertainty is ±5% in HRR and ±2 s in time.

Table 1
Provided are the average physical characteristics of CNF/PUF. All values are reported with 2σ standard uncertainty.

Mass (g)	Mass fraction % coating	Mass fraction % CNF		Coating thickness (nm)
		on CNF/PUF	in coating	
13.1 ± 0.4	3.2 ± 0.4	1.6 ± 0.1	51 ± 1	359 ± 36

3. Results and discussion

3.1. CNF coating characterization

According to QCM (Fig. 2) and profilometry (Fig. 3), the coating growth occurs in two stages. Up to three bilayers there is very little increase in mass or coating thickness. Interpolation of this data indicates less than 50 nm thickness and 12 μg/cm^2 after three bilayers. At four bilayers the coating growth rate rapidly increases with each bilayer increasing the coating thickness by 87 nm ± 10 nm. This is consist with qualitative observations during the LbL process where the foam transitioned from a white to a slight gray with the first three bilayers, but became a deep black color and noticeably stiffer after with the fourth bilayer. This two step growth with a small initial growth of the coating is quite common and suggests a weak attraction (perhaps due to a poor surface charge on the foam) between the foam and the LbL polymers. It is assumed the initial depositions result in the formation of island-like coatings wetting the surface of the foam and several bilayers are required before the entire surface is covered by the polymeric coating. The fundamentals of LbL coating on foam and factors influencing the initial coating growth process are currently being investigated.

SEM was used to characterize the LbL fabricated CNF coatings on PUF. The SEM images of the as-received and washed PUF are shown in Fig. 4. The images of the CNF/PUF shown in Fig. 5 are of a section near the center of a CNF/PUF specimen. These images are representative of the type of coating observed on all specimens. The bright white CNFs are those not (or only partially) covered with polymer. The images of the cross section of the coating are provided in Fig. 6 and Fig. 7. Delamination of the coating from the PUF appears to be a rare occurrence, as it was only observed once in many samples analyzed by SEM (Fig. 7). The root cause of this delamination is unknown. One possible explanation is the coating did not adhere to the PUF surface because of the high fiber concentration. Another possibility is the freeze fracture process caused delamination. Regardless of the cause, these images reveal that the coatings have regions of high fiber aggregation welded together with polymer.

Other than dust and debris on the surface of the PUF, the as-received PUF surface appears smooth and featureless even at high magnification (Fig. 4). Prior to depositing the first layer, the PUF was washed with DI water, which completely removed all of the debris (Fig. 4c). The wavy appearance (Fig. 4b) and the extra material

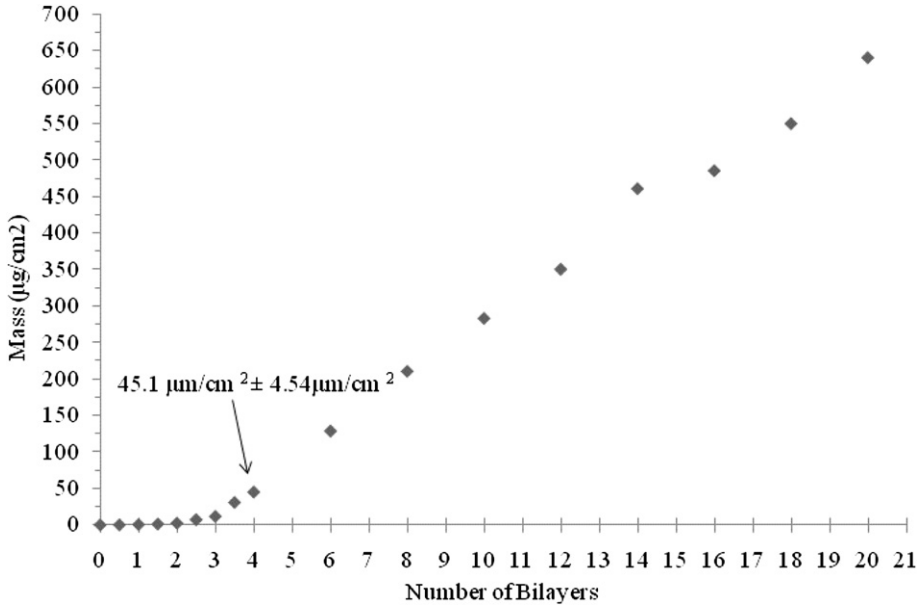

Fig. 2. Coating mass increase on QCM crystal as a function of PEI/CNF:PAA bilayers. Mass increase occurs in two stages. Initially, the coating growth is slow, but between at three bilayers there is a transition to a rapid and linear coating growth over the next 16 to 18 bilayers. The size of the data markers represents the 2σ standard uncertainty of the measured mass.

(Fig. 4c) on the edge of the PUF wall is a result of the manufacturing process. The PUF was initially closed cell with a very thin membrane connecting the walls. When the membrane was "popped" during manufacturing, there was a slight relaxation of the strained edges of the walls and the membrane material snapped back onto the walls, which leaves behind extra material on the edge and creates a wavy appearance.

The images in Fig. 5 indicate that the CNFs are well distributed along the walls of the PUF. At low magnification (Fig. 5a), the wall surfaces appear to be sparsely populated, with approximately 10 µm by 10 µm sized aggregates of CNFs. The areas between the aggregates are populated with a network of CNF whiskers and regions that appear to be free of CNFs. At higher magnifications (Fig. 5b and c), it becomes apparent that a portion of these regions actually do contain CNFs and these are not visible at lower magnifications because they are embedded in the polymer coating. Along the surface there are also "islands" of CNFs that appear to have dewetted from the surface (Fig. 5b and c). The larger islands (approximately 10 µm) appear to contain more single CNFs, rather than the bundles observed in the larger aggregates (Fig. 5d).

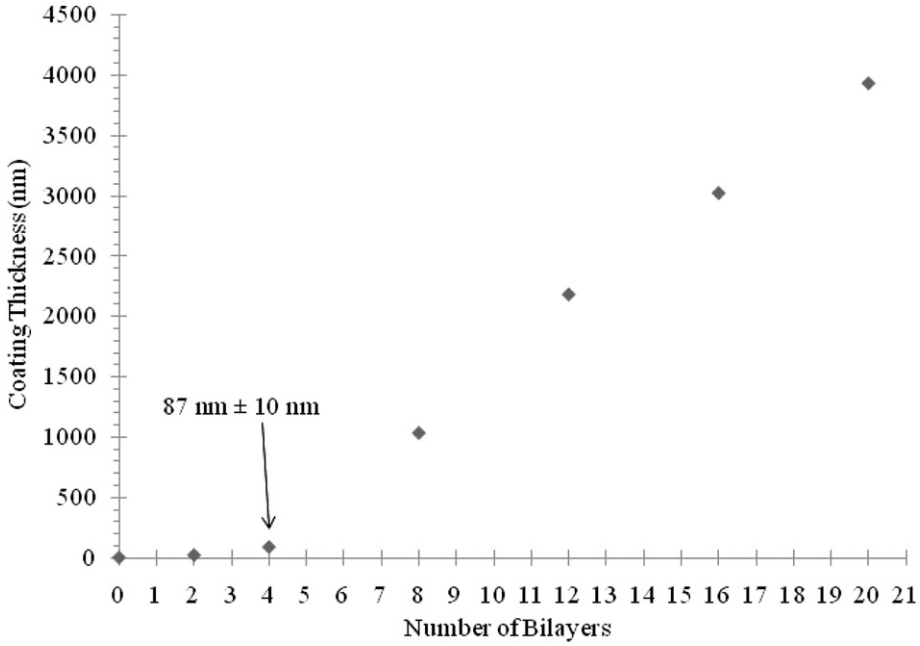

Fig. 3. Profilometer measurements of the CNF coating thickness on a glass slide. Thickness growth follows the same two stage growth observed in the QCM data. The size of the data markers represents the 2σ standard uncertainty of the measured thickness.

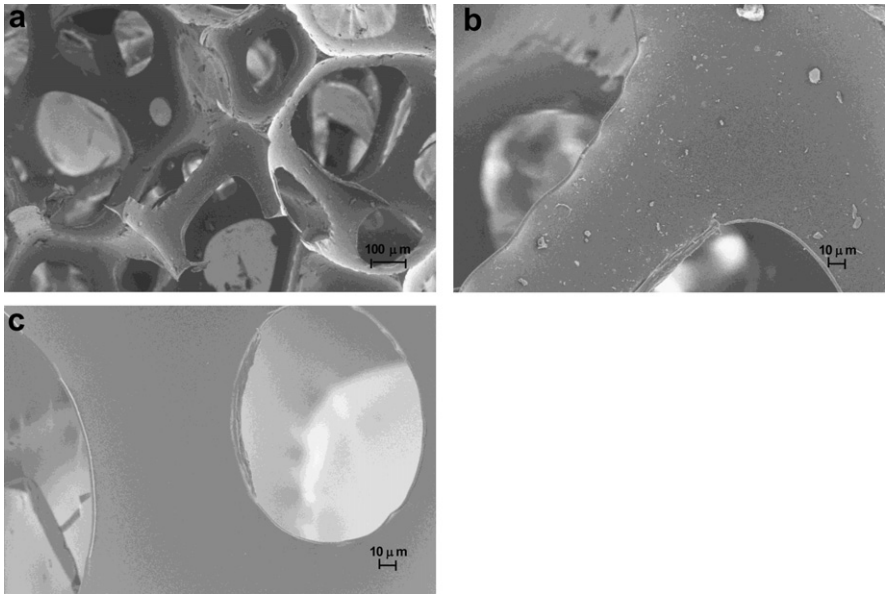

Fig. 4. SEM images of as-received PUF at (a) 1,000x and (b) 5,000x and (c) washed PUF at 5,000x. The wall surface was smooth and featureless. The edges of some struts are wavy due to recoiling of material from breaking the membrane and/or shrinkage due to solvent loss during the PUF manufacturing.

The smaller islands (less than 3 μm) either contain no CNFs or what appears to be short individual CNFs (less than 1 μm).

SEM images of a fractured CNF/PUF were taken with the fracture surface in the plane of the image, which provides cross section views of the PUF and the coating (Fig. 6). The CNF coatings are 359 nm ± 36 nm (based on 10 measurements of five different CNF/PUF specimens (Fig. 6c), which is 272 nm thicker than measured by the profilometer (Fig. 3). The profilometer values (Fig. 3) best represent the trend in the coating deposition, but not the actual values because LbL coatings are thicker on a porous three dimension substrate than on a flat slide [26,32]. The surface morphology at low magnification (Fig. 6a) is consistent with that observed in Fig. 5 (large aggregates, CNF network, and areas without CNF). Based on all the images taken of fractured CNF/PUFs, the CNF coating appears to cover the entire surface; although, the thickness is not completely uniform.

The thicker islands, one of which is shown in Fig. 6b, are 374 nm ± 100 nm and are constructed of at least twenty CNF fibers randomly oriented in the plane of the coating. The "hills and valleys" topography of the islands are created by overlapping CNFs. The fairly uniform (34 nm ± 2 nm) polymer coating covering the CNFs, and the small gaps between them, suggest that these fibers were probably deposited at the same time. Analysis of other islands reveals similar characteristics, which suggests the fibers in the islands were probably deposited as loosely interacting groups rather than isolated and independent CNFs. The last layer of polymer covering the CNFs varied from island to island, but never exceeded 34 nm ± 2 nm. This is the same thickness measured for the regions between the thicker

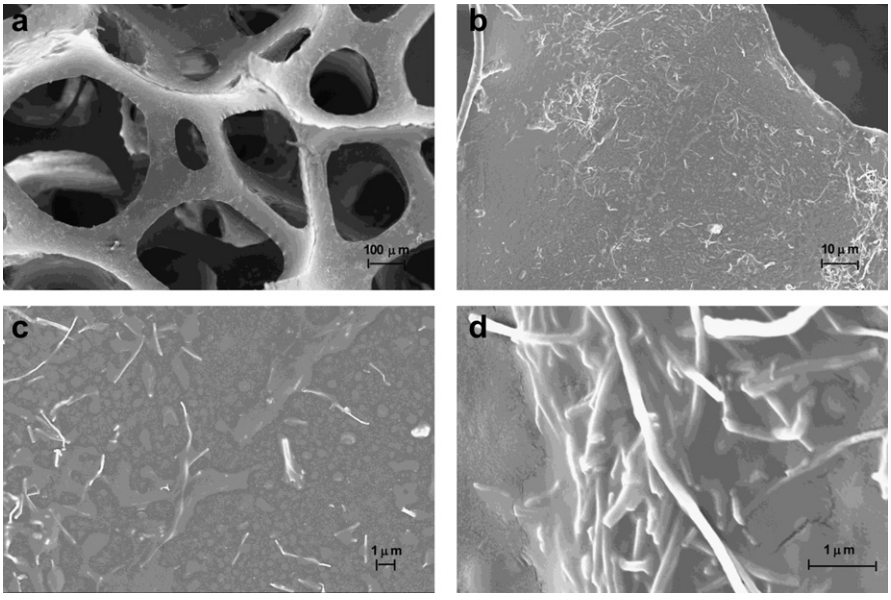

Fig. 5. SEM images of the inside section of a CNF coated PUF at (a) 1,000x and (b) 10,000x, (c) of thicker islands at 50,000x, and (d) of an aggregate at 200,000x.

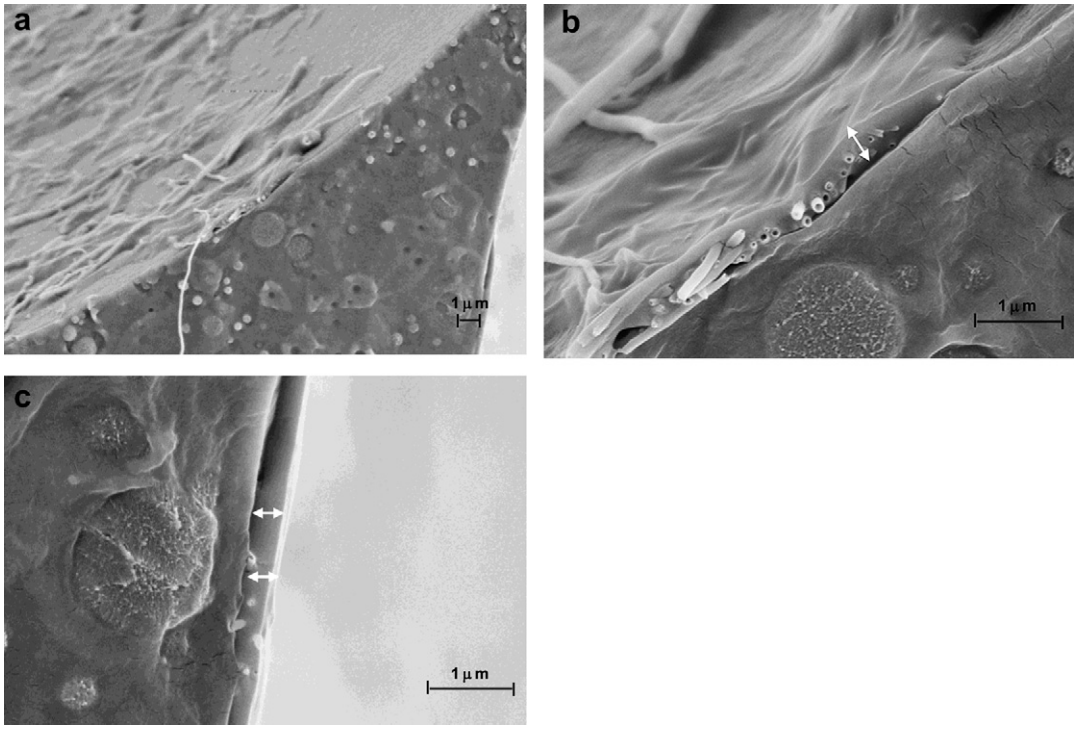

Fig. 6. SEM images of a fractured edge of CNF coated PUF at (a) 50,000x, (b) a thicker island at 200,000x, and (c) a typical 359 nm ± 36 nm coating at 200,000x. The thinner region near the top edge of (a) appeared to contain little or no CNFs (34 nm ± 2 nm). The values are reported with 2σ standard uncertainty.

islands, which appear to contain little to no CNFs. Fig. 7 is the only example of coating delamination. The delamination may have resulted from the freeze fracture process or may indicate a section of poor adhesion. These images illustrate that the coating can contain regions of high CNF concentration welded together by polymer.

3.2. CNF/PUF thermal analysis and fire performance

TGA and a microbalance were used to determine the actual mass of CNFs and coating deposited onto the substrates. The four BL CNF coating increases the mass of the substrate by 3.2 mass fraction % ± 0.4 mass fraction %, of which, 51 mass fraction % ± 1 mass fraction % are CNFs. The total CNF content relative to the substrate mass is 1.6 mass fraction % ± 0.1 mass fraction %, which is a typical loading level of carbon nanotubes or nanofibers incorporated into polymers (not a coating) to improve the polymer's fire resistance. Unlike these other nanocomposites, the CNFs in these coatings are concentrated at the surface rather than randomly dispersed and distributed throughout the polymer matrix [27,30].

Cone Calorimetry (Cone) is a routine bench scale fire test that simulates a developing fire scenario on a small specimen and is used to measure the forced burning fire performance of polymers. The parameters reported from the test, such as time to ignition of the combustion gases (TTI), the time to peak and the peak maximum heat release rate (PHRR), and the total heat release (THR), are directly related to the potential fire threat of the burning polymer. The values of these parameters are the bases of the performance metrics for several existing or proposed national fire regulations. The Cone heat release rate measurements are referenced to sample surface area (kW/m^2), which is measured prior to the experiment. As described by Zammarano et al. [33], it is imporatant to normalize the data according to surface area because the PUF samples rapidly form a melt pool, whereas the, CNF filled PUF did not collapse and maintained an approximate two times larger surface area during the test. The data presented here, however, was not normalized in terms of surface area (discussed below).

The HRR data indicates the CNF coatings significantly improved the fire resistance of foam (Fig. 8, Table 2 and Table 3). The HRR curves for CNF/PUF and PUF consist of two peaks. However, the attributes of the curves are quite different with both peaks of CNF/PUF being of similar HRR values (371 kW/m^2 ± 10 kW/m^2 and

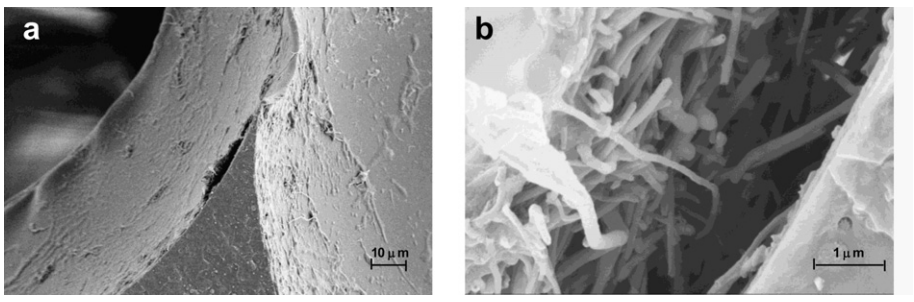

Fig. 7. SEM images of a delaminated CNF coating on PUF at (a) 10,000x and (b) 200,000x. The heavy concentration of CNFs below the surface was welded together with polymer.

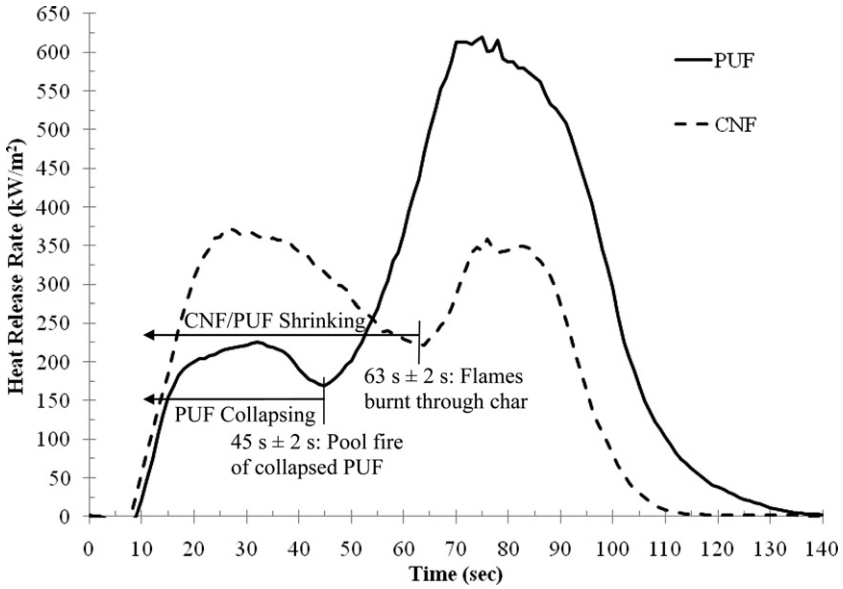

Fig. 8. Heat Release Rate curves of the washed standard PUF and the CNF/PUF indicates the CNF coating significantly improved the fire performance of the PUF (e.g., 40% ± 3% reduction in PHRR). The ability of the CNF coating to promote char formation and prevent the foam from collapsing into a pool are assumed to be the primary reasons for the measured reduction in PHRR, THR, and total burn time.

348 kW/m^2 ± 10 kW/m^2) whereas in PUF the second peak is 2.8 times larger than the first peak (224 kW/m^2 ± 12 kW/m^2 and 620 kW/m^2 ± 26 kW/m^2). The PHRR, which is often considered as one of the more critical values in accessing the flammability of a material, is 40% ± 3% lower for CNF/PUF than for PUF. The THR, which reflects the total size of the fire threat, and the total burning time of the foam was 21% ± 3% smaller for CNF/PUF. However, the time to PHRR, which is often considered a critical value in accessing the amount of time for escaping a fire, is 66% ± 2% earlier for CNF/PUF. In other words, the Cone data suggests the CNF coatings may result in smaller fires and reduced flame spread, but create an initially larger fire that reduces the time to escape. In a real scenario, the CNF/PUF would likely perform significantly better than the HRR data suggests, but before going into this discussion it important to understand how the CNF coating altered the burning behavior of foam.

The attributes of the first HRR peak for both CNF/PUF and PUF are defined by pyrolysis of polyurethane decomposition gases (increase in HRR) and decrease in substrate surface area (decrease in HRR). During the first peak the CNF coating forms a protective char and enables the foam to maintain its shape (and surface area) that is qualitatively similar to an untested foam specimen. At 63 s ± 2 s, the flames penetrate this protective char, which causes the foam to shrink as the remaining polymer is pyrolyzed. At the end of the experiment, a brittle char remains that has a surface area 90% ± 5% smaller than the untested foam specimen. In contrast to CNF/PUF, during the first HRR peak PUF collapses to form a liquid-like pool of degraded polyurethane. The surface area of this pool (defined by the sample pan) is qualitatively two times smaller than CNF/PUF surface area, which is the reason the HRR maximum for the first peak is 66% ± 2% higher for CNF/PUF. The PUF pool rapidly pyrolyzes because there is no protective char and because the contents of the pool are volatile/combustible compounds (isocyanate and polyol based degradation products of polyurethane).

In a real fire scenario, the reduction in flammability due to replacing PUF with CNF/PUF will likely be greater than suggested by the Cone data (Fig. 8 and Table 2) for two main reasons. First, this CNF/PUF Cone data (Fig. 8 and Table 2) was not normalized, as suggested by Zammarano et al. [33], since the surface area for CNF/PUF was not quantitatively measured and changed significantly throughout the test. Based on the qualitative observations, the HRR for the first peak could be reduced by a factor of two while the second peak may only be slightly reduced. The result is the first peak for CNF/PUF would have a maximum HRR and time to peak similar to PUF and the second peak would then become the PHRR, which has a time to peak similar to PUF. Secondly, the Cone data does not capture the real impact of the PUF pool fire since there is no product for the pool fire to pose an additional flux upon. Since a pool fire can approximately increase the fire threat (as calculated from HRR, THR, and burn time) of a burning product (e.g. upholstered furniture) by 35% [29] and the CNF coating prevents pool formation than it is assumed that in a real fire replacing PUF with CNF/PUF would decrease the HRR from a product by 35%.

3.3. Comparison to other flame retarding technologies

A previous study reported a 35% reduction (Table 3) in PHRR for PUF using 4 mass fraction % CNFs embedded in the PUF (CNFs were

Table 2
Cone Calorimetry data of the PUF and CNF/PUF samples. The CNF coating reduced THR, PHRR, and total burn time, and delayed time to peaks, but increased the PHRR value for the first peak. All values are reported with 2σ standard uncertainty.

	Peak 1		Peak 2		THR (MJ/m^2)	Residue Mass Fraction %	Burn time (s)
	HRR (kW/m^2)	Time (s)	HRR (kW/m^2)	Time (s)			
PUF	224 ± 12	32 ± 2	620 ± 26	75 ± 3	33 ± 2	2.2 ± 0.1	140 ± 2
CNF/PUF	371 ± 10	27 ± 2	348 ± 10	83 ± 2	26 ± 1	11.0 ± 0.4	110 ± 2

Table 3
Reduction of Cone Calorimetry data caused by CNF LbL coating on PUF, CNF embedded in PUF, and commercial FR embedded in PUF. All values are reported as a % reduction relative to the standard PUF used in their study. All values measured in this study are reported with 2σ standard uncertainty. No uncertainty was reported for the literature values.

Reduction as compared to pure PUF		
FR (mass fraction % loading)	PHRR	THR
CNF (1.6% ± 0.1%)	40% ± 3%	21% ± 3%
CNF (embedded) (4%)	34%	
4 Halogen FRs (20%)	31%	16%
5 Non-halogen FRs (4%)	15%	14%
7 Halogen-Phosphorous FRs (28%)	14%	7%

added to the foam recipe) [27]. In comparison, the LbL fabricated CNF/PUF specimen has a 20% greater reduction in PHRR using 57 mass fraction % less CNFs. In other words, incorporating CNF as a coating rather than directly into the polyurethane yields a significantly greater reduction in PUF flammability. This information may be of particular interest to foam manufacturers, as it is assumed the post-manufacturing coating of CNFs and using less CNFs will be easier and more cost effective to implement than incorporating CNFs into the foam recipe.

Najafi-Mohajeri used the Cone to measure the impact of 16 flame retardant additive packages (five non-halogen, four halogen, and seven halogen-phosphorous) on the flammability of a standard PUF [34]. These additive packages are commercially available and reported to be commonly used by the PUF industry. The five non-halogens reduced the PUF PHRR and THR by an average of 15% and 14%, respectively, at a 3.3 mass fraction % averaged loading. The four halogens reduced the PUF PHRR and THR by an average of 31% and 16%, respectively, at a 20 mass fraction % averaged loading. The seven halogen-phosphorous systems reduced the PUF PHRR and THR by an average of 14% and 7%, respectively, at a 28 mass fraction % averaged loading.

Also using a Cone, Price measured the flammability impact of incorporating melamine-based flame retardants into PUF [35]. The exact composition of the materials is unknown as they were purchased from a supplier. The melamine and melamine chlorate phosphate blend reduced the PHRR by 10% and 15%, respectively. As an alternative to using flame retardants, the authors also measured the impact of using fire blocking barrier fabrics to reduce the PUF flammability. Of the six specimens tested, the best performing combination was wrapping the standard PUF with zirconium hexafluoride flame retardant treated wool (FR-wool), which gave a 29% reduction in PHRR. This FR-wool also gave the greatest reduction in PHRR of the flame retardant foams (32%), which was quite similar to what was reported for wrapping the standard PUF with this FR-wool. These results suggest the fire performance benefits gained by using these flame retardants are partially mitigated by the FR-wool.

Compared to these competitor flame retardant (FR) systems, the CNF coatings developed in this project delivered a 14%–65% larger reduction in PHRR and THR using 46%–95% less FR [34,35]. Normalizing based on FR content, the per mass fraction % FR reduction in HRR was larger for the CNF coating by

- 38% compared to CNF embedded,
- 288% compared to halogen FRs,
- 158% compared to non-halogen FRs, and
- 1138% larger compared to halogen-phosphorous FRs.

The 20% larger reduction as compared to FR-wool barrier fabric system was not normalized because the FR content was not reported.

4. Conclusions

For the first time, LbL assemblies made with CNFs are shown to improve the fire performance of polyurethane foam. The process described here generates thin film coatings that completely cover all internal and external surfaces of the porous polyurethane foam. Even though the CNF distribution is not completely uniform, and the CNFs are not completely embedded in the polymer coating, the coating significantly reduces the flammability of foam. This LbL coating significantly reduces the heat release rate, total heat release, and total burn time of the PUF with just four bilayers (e.g., 40% ± 3% reduction in PHRR). Compared to FR systems currently used to reduce PUF flammability, and embedding the CNFs directly into PUF, these CNF-based coatings yield a significantly greater reduction in PUF flammability at a significantly lower additive concentration (e.g., 1.6 mass fraction % CNF coating on PUF yields a 23% lower PHRR than a 20 mass fraction % brominated FR in PUF). Normalizing according to FR content, the reduction in foam HRR is 38%–1138% greater for these CNF coatings than these alternatives FR systems. The CNF coating also prevents the formation of a melt pool of burning foam, which in a real fire scenario, may further reduce the resulting fire threat of burning soft furnishings in residential homes. This research lays the foundation for using LbL to fabricate coatings on foam and barrier fabrics using a range of nanoparticles and other performance-enhancing additives. Multi-walled carbon nanotubes, clay, cellulosic fibers, and mixed additive coatings are currently being investigated on both foam and barrier fabrics. Additionally, the release of nanoparticles during aging and the change in fire performance due to aging are currently being measured.

Acknowledgements

The authors thank Professor Alexander Morgan at University of Dayton Research Institute for cone calorimeter testing.

References

[1] Hall JR. Total cost of fire in the United States. National Fire Protection Association Report; 2010.
[2] Hall JR, Harwood B. Fire Technology 1989;25(2):99–113.
[3] Miller D, Chowdhury R, Greene M. 2005-2007 residential fire loss estimates. Consumer Product Safety Commission report; 2010.
[4] Ahrens M. Home fires that began with upholstered furniture. National Fire Protection Association; 2008.
[5] 16 CFR 1632 Standard for the flammability of mattresses and mattress pads. Consumer Product Safety Commission; 1991.
[6] 16 CFR 1633 Standard for the flammability (open flame) of mattress sets. Consumer Product Safety Commission; 2006.
[7] 16 CFR 1634 Standard for the flammability of residential upholstered furniture. Consumer Product Safety Commission; 2008.
[8] http://echa.europa.eu/reach_en.asp, [last accessed on 02. 02. 2011].
[9] http://ec.europa.eu/environment/ecolabel/, [last accessed on 02. 02. 2011].
[10] Decher G. Polyelectrolyte multilayers, an overview. In: Decher G, Schlenoff JB, editors. Multilayer thin films: Sequential assembly of nanocomposite materials. Weinheim, Germany: Wiley-VCH; 2003 [chapter 1].
[11] Podsiadlo P, Shim BS, Kotov NA. Coordination Chemistry Reviews 2009; 253(23–24):2835–51.
[12] Li YC, Schulz J, Mannen S, Delhom C, Condon B, Chang S, et al. Acs Nano 2010; 4(6):3325–37.
[13] Shimazaki Y, Nakamura R, Ito S, Yamamoto M. Langmuir 2001;17(3):953–6.
[14] Lv F, Peng ZH, Zhang LL, Yao LS, Liu Y, Xuan L. Liquid Crystals 2009;36(1): 43–51.
[15] Bergbreiter DE, Chance BS. Macromolecules 2007;40(15):5337–43.
[16] Mermut O, Barrett CJ. Journal of Physical Chemistry B 2003;107(11): 2525–30.
[17] Chang L, Kong XX, Wang F, Wang LY, Shen JC. Thin Solid Films 2008;516(8): 2125–9.
[18] Priolo MA, Gamboa D, Grunlan JC. Acs Applied Materials & Interfaces 2010; 2(1):312–20.
[19] Aoki PHB, Volpati D, Riul A, Caetano W, Constantino CJL. Langmuir 2009; 25(4):2331–8.

[20] Fu JH, Ji J, Fan DZ, Shen JC. Journal of Biomedical Materials Research Part A 2006;79A(3):665–74.
[21] Hiller J, Mendelsohn JD, Rubner MF. Nature Materials 2002;1(1):59–63.
[22] Davis RD, Gilman JW, VanderHart DL. Polymer Degradation and Stability 2003;79(1):111–21.
[23] Gilman JW, Bourbigot S, Shields JR, Nyden M, Kashiwagi T, Davis RD, et al. Journal of Materials Science 2003;38(22):4451–60.
[24] Davis RD, Lyon RE, Takemori MT, Eidelman N. High throughput techniques for fire resistant materials development. In: Wilkie CA, Morgan AB, editors. Fire retardancy of polymeric materials. Boca Raton, FL: Tayler & Francis Group; 2010 ([chapter 16]).
[25] Podsiadlo P, Michel M, Lee J, Verploegen E, Kam NWS, Ball V, et al. Nano Letters 2008;8(6):1762–70.
[26] Li YC, Schulz J, Grunlan JC. Acs Applied Materials & Interfaces 2009;1(10): 2338–47.
[27] Zammarano M, Kramer RH, Harris R, Ohlemiller TJ, Shields JR, Rahatekar SS, et al. Polymers for Advanced Technologies 2008;19(6):588–95.
[28] Tibbetts GG, Lake ML, Strong KL, Rice BP. Composites Science and Technology 2007;67(7–8):1709–18.
[29] Pitts WM, Hasapis G, Macatangga P. Fire spread and growth on flexible polyurethane foam. Eastern States Section of the Combustion Institute. College Park: Maryland; 2009.
[30] Kashiwagi T, Du FM, Douglas JF, Winey KI, Harris RH, Shields JR. Nature Materials 2005;4(12):928–33.
[31] Drysdale D. An introduction to fire dynamics. 2nd ed. West Sussex, England: John Wiley & Sons Ltd; 1999.
[32] Davis RD, Kim YS. Fabrication, characterization and flammability testing of carbon nanofiber layer-by-layer coated polyurethane foam. National Institute of Standards and Technology Technical Report 1674. National Institute of Standards and Technology; 2010.
[33] Zammarano M. Foam flammability. 2008 annual fire Conference. Gaithersburg, MD: National Institutue of Standards and Technology; 2008.
[34] Najafi-Mohajeri N, Jayakody C, Nelson GL. Cone calorimetric analysis of modified polyurethane elastomers and foams with flame-retardant additives. In: Nelson GL, Wilkie CA, editors. Fire and polymers: materials and solutions for hazard prevention. Washington, DC: American Chemical Society; 2001.
[35] Price D, Liu Y, Hull TR, Milnes GJ, Kandola BK, Horrocks AR. Polymer International 2000;49(10):1153–7.